Security of Infocommunication Systems and Internet of Things

2025 Vol 3, No 1

https://doi.org/10.31861/sisiot2025.1.01006

Received 24 May 2025; revised 17 June 2025; accepted 20 June 2025; published 30 June 2025

Interference-based Research of the Goos-Hänchen Effect

Petro Maksymiak and Serhii Shchukin*

Department of Correlation Optics, Yuriy Fedkovych Chernivtsi National University, Chernivtsi, Ukraine

*Corresponding author (E-mail: shchukin.serhii@chnu.edu.ua)

ABSTRACT The paper provides an overview of the Goos-Hänchen effect, which demonstrate that upon total internal reflection of a polarized beam, longitudinal shifts of the beam occur, differing for various polarizations. These shifts must be taken into account when a beam propagates through an optical fiber, as in a fiber-optic communication system, total internal reflection of the beam occurs at the core-cladding interface of the fiber. The paper presents a novel method for measuring longitudinal Goos-Hänchen shifts, which is based on three-beam interference. Using an experimental setup that implements this method, it was possible to measure the phase shifts of orthogonal beams separately. It was established that during the total internal reflection of coaxial, orthogonally linearly polarized beams, there is no change in the phase difference between these beams, even in the presence of the Goos-Hänchen effect. This result suggests the feasibility of the simultaneous use of orthogonally linearly polarized beams in fiber-optic communication lines and provides a positive prognosis for such applications.

KEYWORDS Goos-Hänchen effect, total internal reflection, orthogonal polarizations, fiber optic communication lines, polarizer.

I. INTRODUCTION

Optical fiber is an invaluable part of fiber-optic communications lines (FOCL). An important task in designing FOCL is to turn the disadvantages of optical fiber into advantages. Utilizing these advantages in fiber-optic communication systems will allow for increased transmission speed while reducing errors.

When a beam propagates through an optical fiber in a fiber-optic communication system, total internal reflection (TIR) of the beam occurs at the interface between the core and the cladding of the optical fiber.

Goos and Hänchen (1947) showed that upon TIR of a linearly polarized beam, a longitudinal shift of the beam occurs, which is different for orthogonal polarizations [1].

Fedorov theoretically predicted it in 1955 and Imbert experimentally demonstrated in 1972 that upon TIR of circularly polarized beams, a transverse shift occurs (orthogonally polarized beams shift in opposite directions) [2, 3].

Consequently, when a beam of arbitrary polarization propagates in an optical fiber, deformation, dispersion, and blurring of this beam occur. In addition to the transverse shift between beams with orthogonal polarizations, there is also their angular displacement [4]. This displacement is due to the Gaussian nature of the beams and depends on the half-width of its Gaussian distribution.

Spatial shifts upon a single TIR of beams are very small – on the order of hundreds of nanometers. They are difficult to measure experimentally because changing beam parameters, particularly polarization, can cause its displacement due to the rotation of imperfect optical elements. Goos and Hänchen used multiple reflections, but later a measurement method [5] was proposed that requires only one reflection.

Recently, numerical analysis has been used to study the regions of validity of analytical formulas that define the displacement of orthogonally polarized beams [6]. In 2016, De Leo et al. found analytical formulas for the Goos-Hänchen (GH) shift of the point of maximum intensity of a Gaussian beam, as well as for the shift of its average intensity [7]. However, near the critical angle, a Gaussian beam is not symmetrical [8, 9], and the point of maximum intensity does not coincide with the average intensity. During a detailed study of the influence of this symmetry breaking of the GH shift, an oscillatory behavior of the curves was revealed [10], the so-called composite GH shift. It is interesting to note that this new phenomenon was missed in previous works due to the assumption of non-divergent beams [11]. Reference [12] investigates the coherent control of the GH shift for a reflected light beam in a double-prism structure, where the space between the prisms is filled with a coherently driven, three-level Raman-gain atomic medium. The GH effect is also being intensively investigated in the radio-frequency range [13].

The aim of our work is to develop an interferometric method for measuring phase shifts between orthogonal polarizations upon TIR, which increases the accuracy of measuring the displacement of polarized beams upon TIR.

II. THREE-BEAM INTERFERENCE SYSTEM

Interferometric methods typically use the mutual interference of two beams, resulting in a sinusoidal intensity as a function of the phase difference, and a shift of interference maxima when an additional path difference is introduced [14].

The interference of three, four, or more beams changes the nature of the aforementioned dependencies and, in several cases, can offer advantages over two-beam interference in terms of sensitivity, measurement accuracy, or other characteristics.

In our research, we used a three-beam interferometer setup [13].

A three-beam interference system can be implemented, for example, based on a three-slit Young's scheme. Fig. 1

shows an optical setup that allows for the observation of three-beam interference. Objective O_1 forms a parallel beam of rays from source S_1. The parallel beam of rays passes through diaphragm S_2, which has three slits equidistant from each other. This results in Fraunhofer diffraction and mutual interference of the beams. The interference result can be observed in the focal plane of objective O_2.

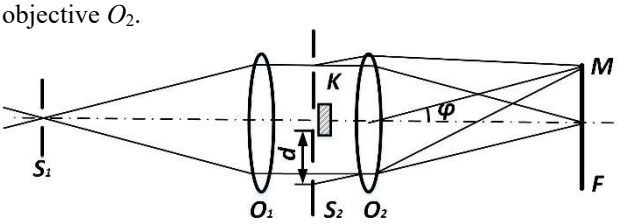

FIG. 1. Scheme for observing three-beam interference. S_1 – source, O_1, O_2 – objectives, S_2 – three-slit diaphragm, K – plane-parallel plate, F – focal plane, M – observation point, ϕ – diffraction angle, d – distance between slits.

Let $a1 = a2 = a3 = a$ be the amplitudes of the light oscillations of the beams emerging from each slit. Since the distance between the slits is the same and equal to d, one extreme beam arrives at a certain point M of the interference field with a phase lead (δ) compared to the middle beam, and the other with the same lag ($-\delta$). The phase shift, determined by the outer slits relative to the middle one, is defined by the relation:

$$\delta = \pm kd\sin\varphi, \tag{1}$$

where $k = 2\pi/\lambda$, and d is the path difference corresponding to point M on the screen; φ is the diffraction angle.

Let's represent the expressions for the three light oscillations in complex form, without considering the time dependence:

$$\begin{aligned} S_1 &= ae^{-i[(2\pi/\lambda)l+\delta]}; \\ S_2 &= ae^{-i[(2\pi/\lambda)l]}; \\ S_3 &= ae^{-i[(2\pi/\lambda)l-\delta]}. \end{aligned} \tag{2}$$

Here l is the optical path length of the middle beam. The resulting light oscillation will be:

$$S_\Sigma = S_1 + S_2 + S_3 = ae^{-i[(2\pi/\lambda)l]}\left(e^{-i\delta} + 1 + e^{+i\delta}\right) = ae^{-i(2\pi/\lambda)l}(1 + 2\cos\delta). \tag{3}$$

The corresponding expression for intensity is found by multiplying S_Σ by its complex conjugate:

$$I = S_\Sigma S_\Sigma^* = a^2(1 + 2\cos\delta)^2. \tag{4}$$

Through trigonometric transformations, we obtain:

$$I = a^2\frac{[\sin 3(\delta/2)]^2}{[\sin(\delta/2)]^2}. \tag{5}$$

Expression (5) is typical for the diffraction of three beams. Graphically, dependence (5) is shown in Fig. 2. The interference pattern is an alternation of principal and secondary maxima at corresponding specific values of δ.

Now, let some additional optical path length be introduced into the path of the middle beam, for example, a plane-parallel plate K (see Fig. 1). The light oscillation corresponding to the middle beam acquires an additional phase $\beta' = (2\pi/\lambda)\Delta'$, where $\Delta' = d'(n' - 1)$, (d' is the thickness of plate K, n' is its refractive index).

The resulting oscillation will be:

$$S'_\Sigma = ae^{-i(2\pi/\lambda)l}\left(e^{-i\delta} + e^{-i\beta'} + e^{+i\delta}\right). \tag{6}$$

The corresponding intensity is obtained by multiplying both parts of the equality by the complex conjugate expression:

$$I = S'_\Sigma S'^*_\Sigma = a^2(1 + 4[\cos\delta]^2 + 4\cos\delta\cos\beta'). \tag{7}$$

Graphically, distribution (7) is presented in Fig. 2 for different β. Introducing an additional phase β into the middle beam leads not to a shift of the interference fringes, as observed in two-beam interference, but to a redistribution of intensities while the positions of the extrema remain unchanged.

Let's explain this. When $\beta = 2\pi n$ ($n = 0,1,2,\dots$), expression (7) coincides with (4). In this case, as δ changes, an alternation of principal and secondary maxima is observed (Fig. 2a). When $\beta = (2n + 1)\pi/2$, the intensity will be determined by the expression:

$$I = a^2(1 + 4[\cos\delta]^2). \tag{8}$$

The intensity distribution in this case, as δ changes, is shown in Fig. 2b. Here, the intensities of the principal and secondary maxima become equal and are approximately half of the maximum intensity, which in Fig. 2a is equal to one. The contrast of the interference pattern somewhat deteriorates because the intensity according to (8) does not reach zero for any values of δ.

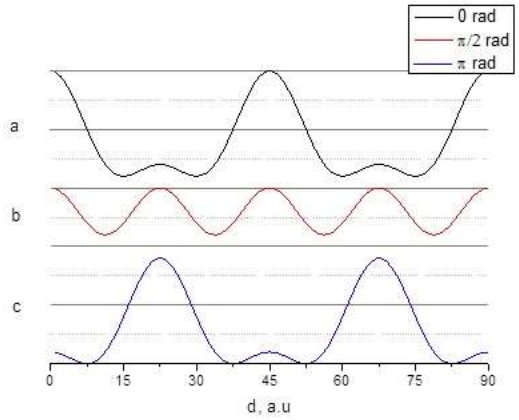

FIG. 2. The resulting intensity pattern from the interference of three beams for specific phase differences between the side beams and the middle beam: (a) 0 radians, (b) $\pi/2$ radians, and (c) π radians.

When $\beta = (2n + 1)\pi$, expression (7) takes the form:

$$I = a^2(1 - 2\cos\delta)^2. \tag{9}$$

As can be seen from (9), the nature of the intensity distribution remains the same as in the case of Fig. 2a, the difference being that the principal and secondary maxima swap places, as seen in Fig. 2c. When comparing analytical expressions (4), (8), and (9), it is evident that expressions (4) and (9) are obtained from relation (8) by adding and subtracting the value $4\cos\delta$. Intermediate changes in the additional phase β lead to the addition and subtraction of a smaller cosine ordinate. The additional phase β leads to a redistribution of intensity between the principal and secondary maxima. This circumstance is characteristic of the three-beam type of interference. The accuracy of measuring phase differences in this case will be determined by the accuracy of establishing the equality of intensities

of two adjacent interference fringes. This precision is quantified by the relative intensity difference between those fringes $\Delta I/I$. Assume that the change in intensity ΔI occurred due to a small change in phase $\Delta\beta$ at the position corresponding to the middle curve (Fig. 2b). If the intensities of adjacent interference fringes can be measured with an accuracy of 5%, then the change in optical path difference $\Delta\delta$ can be measured with an accuracy of up to $(1/100)\lambda$.

III. HIGH-PRECISION INTERFEROMETRIC METHOD FOR MEASURING PHASE SHIFTS

We propose a method for measuring the relative phase shifts between orthogonal linearly-polarized beams upon TIR. The method is based on three-beam interference, a key feature of which is the formation of an interference pattern in the focal plane of a lens, appearing as a harmonic intensity distribution with distinct amplitude extrema. The period of the interference in this case is determined by the separation of the outer slits. A change in the phase of the central beam – that is, its displacement along the direction of propagation – leads to a redistribution of the extrema in the interference pattern. For clarity, we demonstrate how the longitudinal GH shift and the phase shifts that accompany this effect are obtained in Fig. 3.

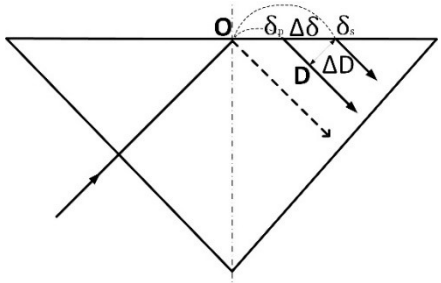

FIG. 3. Schematic of the longitudinal Goos-Hänchen shift.

Coaxial, orthogonally linearly polarized beams are incident on a prism: a P-polarized beam (in the plane of incidence) and an S-polarized beam (perpendicular to it). Due to the GH effect, the beams experience a spatial shift upon reflection, causing them to emerge at points different from the initial point of incidence, O.

Using the three-beam interferometer, we can measure the phases of the P- and S-polarized beams at their respective exit points, δ_p and δ_s. In the resulting right-angled triangle $\delta_p\delta_s D$, the side $\delta_s D$ corresponds to the GH shift, denoted as ΔD. Considering that triangle $\delta_p\delta_s D$ is an isosceles right-angled triangle, ΔD can be obtained using the following formula:

$$\Delta\delta D = \frac{\lambda\Delta\delta}{2\sqrt{2}\pi}. \qquad (10)$$

We propose a method for measuring relative phase shifts between orthogonally linearly polarized beams upon TIR based on three-beam interference. We measured the relative shift upon TIR between orthogonally linearly and circularly polarized beams in the setup shown in Fig. 4. An important feature of the setup is the creation of an interference pattern by identically polarized beams, which serves as a reference for evaluating the relative shift of the third beam with orthogonal polarization. This setup is a three-beam analog of the classic Young's scheme.

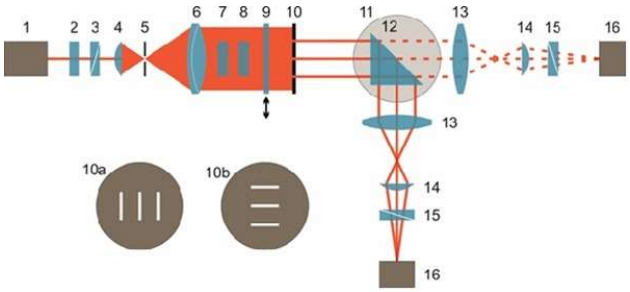

FIG. 4. Scheme of experimental investigations. 1 – single-mode He-Ne laser; 2 – quarter-wave plate; 3 – linear polarizer; 4 – micro-objective; 5 – micron diaphragm; 6 – objective; 7 – half-wave plate; 8 – phase compensator; 9 – quarter-wave plate; 10a, 10b – diaphragm with vertical and horizontal slits; 11 – goniometer; 12 – prism; 13 – objective; 14 – micro-objective; 15 – linear polarizer; 16 – CCD camera. The dashed line shows another arm of the interferometer, which operates in the forward direction, for measuring the phase front of the beams.

The setup is built around a 50 mW, single-mode He-Ne laser (1) providing coherent light at $\lambda = 633$ nm. The initial polarization state is set by a quarter-wave plate (2) and a linear polarizer (3), which together generate a beam with a well-defined linear polarization. To ensure high beam quality, the light is spatially filtered and expanded by a telescopic beam expander. This consists of a micro-objective (4), a pinhole (5), and a collimating lens (6), which collectively produce a plane wave with very high uniformity (wavefront distortion $< \lambda/20$). This plane wave is incident upon a three-slit diaphragm (10). The three identical slits are equidistant and can be oriented horizontally (10a) or vertically (10b) by rotating the diaphragm. To control the beam properties after the slits, a half-wave plate (7) was used to rotate the polarization of the central beam, making it orthogonal to the side beams. Phase compensator 8 allowed for setting an arbitrary phase difference between the orthogonally polarized beams.

The source of optical radiation was a single-mode He-Ne laser 1 with a wavelength $\lambda = 0.6328$ μm and power $P = 50$ mW. A quarter-wave plate 2 and a linear polarizer 3 allowed for the formation of a linearly polarized beam with the required polarization azimuth. The high quality of micro-objective 4 (3x), micro-diaphragm 5 (30 μm), and objective 6 ($f = 63$ cm), which form a telescopic system, allowed for the formation of a plane wave with wavefront irregularities less than $\lambda/20$. The plane wave was incident on a diaphragm consisting of three identical slits, located at strictly equal distances from each other. The slits can be oriented horizontally (10a) or vertically (10b) by rotating diaphragm 10 by 90°. The slit diaphragm was rotated to switch between horizontal and vertical orientations without making mechanical contact with the lens mount, thereby preserving the uniformity of the optical field in both amplitude and phase. A $\lambda/2$ plate (7) was used to convert the polarization of the central beam to a polarization orthogonal to that of the side beams. Phase compensator 8 allowed for setting an arbitrary phase difference between the orthogonally polarized beams.

A $\lambda/4$ plate (9), which can be inserted and removed, converted linearly orthogonally polarized beams into circularly polarized beams with opposite handedness. Then, total internal reflection of the three beams occurred

from the diagonal face of prism (12), mounted on a goniometer stage (11). The refractive index of the prism for the wavelength λ = 633 nm is n = 1.515. The requirements for the flatness of the prism surfaces are also very high. In our case, their flatness was no worse than λ/25.

Subsequently, the Fraunhofer diffraction and the resulting interference of the three reflected beams were observed at the focal plane of objective (13) $f = 38$ cm using a micro-objective (14) and a CCD camera (16). The contrast of the interference pattern was maximized with polarizer 15, which was oriented at an azimuth of 45° relative to the polarization planes of the orthogonally linear polarized beams.

If you remove prism 12, you can observe the diffraction and interference of the three beams in the direct beam path (indicated by dashed lines in Fig. 4). This allows for the proper alignment of the setup's components.

IV. EXPERIMENT

Figure 2 presents the computer-simulated intensity distribution for a three-beam interference pattern. When all beams share the same phase, the resulting pattern is shown in Fig. 2a. Introducing a π/2 phase shift to the central beam relative to the side beams produces the distribution seen in Fig. 2b. If the phase shift is increased to π, the maxima and minima of the interference pattern are interchanged, as illustrated in Fig. 2c.

V. SETUP CALIBRATION

In the preliminary phase of the research, the experimental setup was calibrated. For this calibration, half-wave plate 7 and quarter-wave plate 9, phase compensator 8, and prism 12 were removed from the direct beam path, and an interference image was obtained at the focus of objective 13 (Fig. 5).

As seen in the figure, the horizontal (a) and vertical (b) interference patterns are indistinguishable from one another.

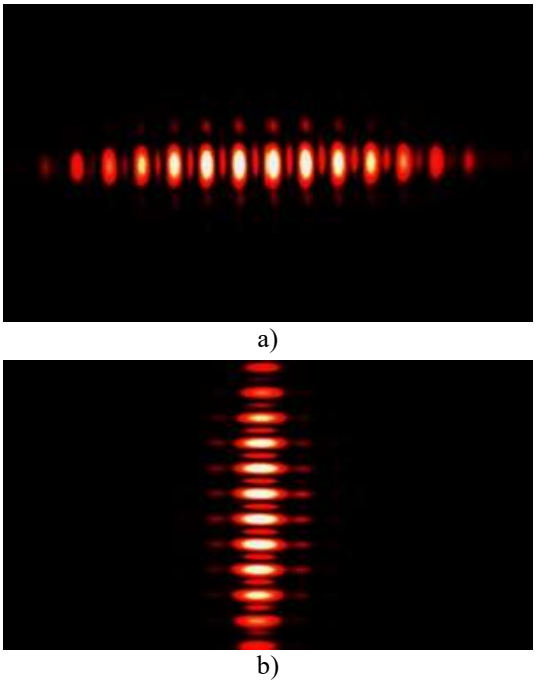

a) b)

FIG. 5. Interference patterns observed at the focal plane of an objective lens, corresponding to (a) horizontally and (b) vertically oriented slits.

Their appearance, corresponding to a zero phase difference between the three beams (Fig. 5a), indicates that the interferometer's illumination channel is accurately aligned.

Next, we insert the λ/2 plate (7), thereby converting the linear polarization of the central beam to be orthogonal to the linearly polarization of the side beams. The phase compensator (8) is used to correct any phase shift in the middle beam, such as the shift caused by the thickness of the half-wave (λ/2) plate (7).

Figure 6 illustrates how the compensator works by showing the different interference patterns that result from varying the phase difference between the middle and side beams.

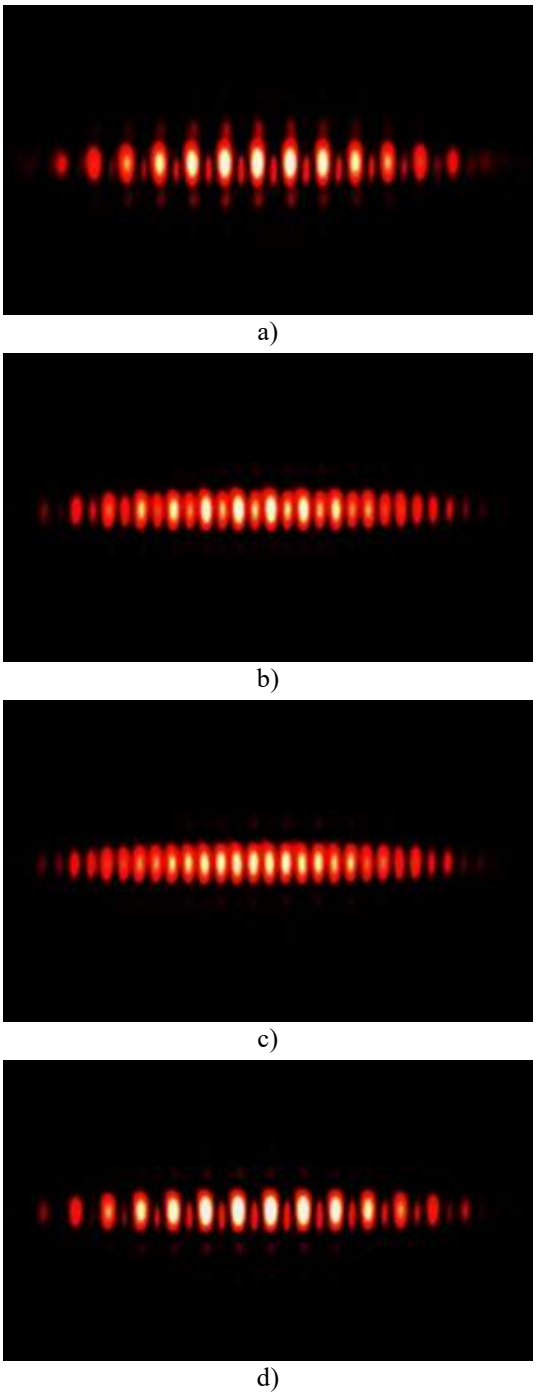

a) b) c) d)

FIG. 6. Interference patterns in three-beam interference for phase differences between the middle and side beams: (a) 0 radians; (b) π/4 radians ; (c) π/2 radians ; (d) π radians.

However, the experiment showed that with a vertical arrangement of diaphragm 10 (slits oriented horizontally) (Fig. 4), when there is no longitudinal shift between beams with orthogonal linear polarizations, and with a horizontal arrangement of diaphragm 10, when a longitudinal shift between the beams exists, the phase difference between the beams coincides (Fig. 7).

The doubling of the interference fringe frequency (Fig. 2b) was established as the reference system for determining the shift caused by the optical path difference between two orthogonally polarized beams. This effect is selected because it provides a more distinct visual marker and is suitable for automated detection.

Rotation of the slits by 90∘ leads to a longitudinal shift between the orthogonal beams; however, this does not change the distribution of the interference pattern (Fig. 8).

Therefore, the phase shift between orthogonally linearly polarized beams does not change when a longitudinal displacement is introduced between them. This result can be explained by the fact that upon total internal reflection, the GH shift also displaces the wavefronts of the reflected, orthogonally linearly polarized beams relative to one another. However, this occurs in such a way that the beams remain in phase, and therefore, the interferometer does not register any longitudinal displacement between them.

This finding indicates that for coaxial, orthogonally linearly polarized beams undergoing total internal reflection, there is no change in the phase difference between them, even in the presence of the GH effect. This, in turn, suggests the feasibility of the simultaneous use of orthogonally linearly polarized beams in fiber-optic communication lines.

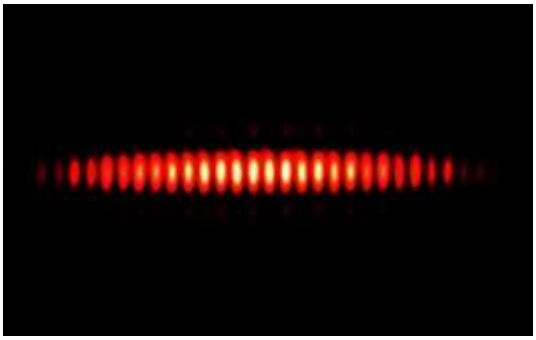

a)

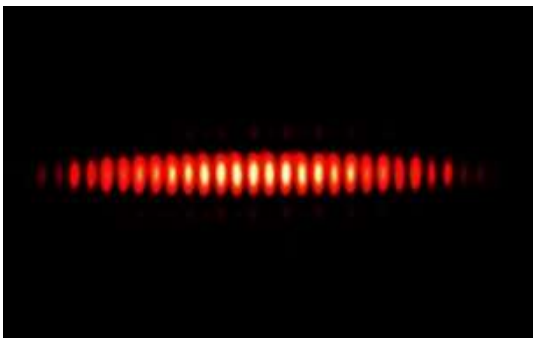

b)

FIG. 7. Three-beam interference patterns produced during total internal reflection using two different diaphragm setups: a vertical one (10a, Fig. 4) and a horizontal one (10b).

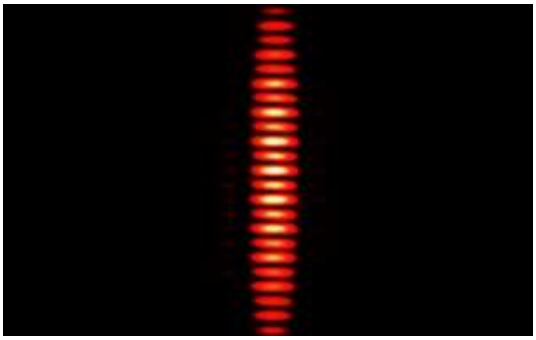

a)

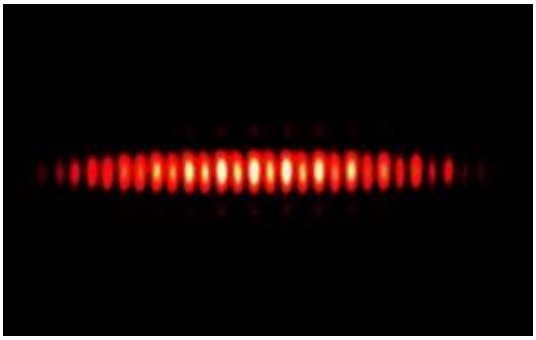

b)

FIG. 8. Interference patterns of three-beam interference upon TIR with vertical arrangement of diaphragm 10 (Fig. 4, 10b), and with horizontal arrangement of diaphragm 10 (Fig. 4, 10a).

However, in this experiment, we were able to determine the absolute phase shifts between orthogonally linearly polarized beams.

For this, we calibrated the setup in the absence of prism 12 (shown in Fig. 1 by dashed lines) and obtained an interference pattern sensitive to the phase difference between orthogonal beams upon TIR for both orientations of diaphragm 10 (Fig. 4).

Compensation of the phase shift using the phase compensator gives us the value of the phase shift, which is 0.66 rad for the horizontal orientation of the diaphragm (Fig. 7a) and 0.67 rad for the vertical orientation (Fig. 8b).

Evaluation of the phase difference between orthogonal beams upon TIR for the parameters of our experiment using the relation:

$$\delta = \delta_p - \delta_s = 2\arctan\left(\frac{cos\theta\sqrt{sin^2\theta - 1/n^2}}{sin^2\theta}\right), \quad (11)$$

gives us a value of 0.69 radians. This is correlates with the experimental results. Using equation (10), we obtain the longitudinal GH shift: $\Delta D = 0.025$ μm.

Our research has the prospect of continuation in interferometric measurements of Goos-Hänchen and Fedorov-Imbert spatial shifts in a modified interferometer.

VI. CONCLUSION

The paper presents an interferometric method developed and implemented by us for measuring phase shifts between orthogonal linear polarizations upon TIR. It was established that upon total internal reflection of coherent orthogonal linearly polarized components, the longitudinal shift between them is not accompanied by a change in the phase difference between these components. This result provides a positive outlook for the simultaneous use of orthogonally linearly polarized beams in fiber optic communication lines.

REFERENCES

[1] F. Goos and H. Hänchen, "Ein neuer und fundamentaler Versuch zur Totalreflexion," *Ann. Phys.*, vol. 436, pp. 333–346, 1947.

[2] F. I. Fedorov, "On the theory of total internal reflection," *Sov. Phys. Dokl.*, vol. 105, pp. 465–468, 1955.

[3] C. Imbert, "Calculation and experimental proof of the transverse shift induced by total internal reflection of a circularly polarized light beam," *Phys. Rev. D*, vol. 5, no. 4, pp. 787–796, 1972.

[4] M. Merano, A. Aiello, M. P. van Exter, and J. P. Woerdman, "Observing angular deviations in the specular reflection of a light beam," *Nat. Photon.*, vol. 3, pp. 337–340, 2009.

[5] H. G. L. Schwefel, W. Köhler, Z. H. Lu, J. Fan, and L. J. Wang, "Direct experimental observation of the single reflection optical Goos-Hänchen shift," *Opt. Lett.*, vol. 33, no. 7, pp. 794–796, 2008.

[6] M. P. Araújo, S. A. Carvalho, and S. De Leo, "The frequency crossover for the Goos-Hänchen shift," *J. Mod. Opt.*, vol. 60, no. 20, pp. 1772–1780, 2013.

[7] M. P. Araújo, S. De Leo, and G. G. Maia, "Closed-form expression for the Goos-Hänchen lateral displacement," *Phys. Rev. A*, vol. 93, no. 2, Art. no. 023801, 2016.

[8] M. P. Araújo, S. A. Carvalho, and S. De Leo, "The asymmetric Goos-Hänchen effect," *J. Opt.*, vol. 16, no. 1, Art. no. 015702, 2014.

[9] M. P. Araújo, S. A. Carvalho, and S. De Leo, "Maximal breaking of symmetry at critical angle and closed-form expression for angular deviations of the Snell law," *Phys. Rev. A*, vol. 90, no. 3, Art. no. 033844, 2014.

[10] M. P. Araújo, S. De Leo, and G. G. Maia, "Oscillatory behavior of light in the composite Goos-Hänchen shift," *Phys. Rev. A*, vol. 95, no. 5, Art. no. 053836, 2017.

[11] H. M. Lai, F. C. Cheng, and W. K. Tang, "Goos-Hänchen effect around and off the critical angle," *J. Opt. Soc. Am. A*, vol. 3, no. 4, pp. 550–557, 1986.

[12] S. Asiri and L. G. Wang, "Controlling the Goos-Hänchen shift in a double prism structure using three-level Raman gain medium," *Sci. Rep.*, vol. 13, Art. no. 22780, 2023.

[13] S. McKay *et al.*, "Observation of a giant Goos-Hänchen shift for matter waves," *Phys. Rev. Lett.*, vol. 134, no. 9, Art. no. 093803, 2025.

[14] M. Born and E. Wolf, *Principles of Optics*. New York, NY, USA: Cambridge Univ. Press, 1999.

Petro Maksymiak

Professor of Correlation Optics Department of Yuriy Fedkovych Chernivtsi National University. Research field: development and implementation of correlation-optical methods of control of roughness of mirror surfaces, diagnostics of random objects, structured light, its research and application.

ORCID ID: 0000-0002-7546-1077

Serhii Shchukin

PhD student at Correlation Optics Department of Yuriy Fedkovych Chernivtsi National University. Research field includes correlation-optical methods, mathematical modelling, telecommunication systems.

ORCID ID: 0009-0009-7144-1560

Інтерференційні дослідження ефекту Гуса-Хенхен

Петро Максимяк, Сергій Щукін*

Кафедра кореляційної оптики, Чернівецький національний університет імені Юрія Федьковича, Чернівці, Україна

*Автор-кореспондент (Електронна адреса: shchukin.serhii@chnu.edu.ua)

АНОТАЦІЯ В роботі розглядається ефект Гуса-Хенхен, який проявляється як поздовжні просторові зміщення поляризованого світлового пучка при повному внутрішньому відбиванні (ПВВ) різні для різних поляризацій. Ці явища є надзвичайно важливими для волоконно-оптичних ліній зв'язку, де передача сигналу відбувається саме завдяки багаторазовим ПВВ пучка на межі між ядром та оболонкою волокна, що може призводити до деформації та розмиття сигналу. Через малу величину зсувів, їх експериментальне вимірювання є складним завданням. Метою даної роботи була розробка та реалізація високоточного інтерференційного методу для вимірювання фазових зсувів, що виникають між ортогонально поляризованими компонентами пучка при повному внутрішньому відбиванні. В основі методу лежить схема трипроменевої інтерференції, яка має суттєву перевагу над двопроменевою: внесення додаткової різниці фаз у центральний пучок призводить не до зміщення інтерференційних смуг, а до перерозподілу їхньої інтенсивності, що дозволяє значно підвищити точність вимірювань. В експериментальній установці використовувався He-Ne лазер, три-щілинна діафрагма, поляризаційні елементи для створення ортогональних поляризацій та призма для здійснення повного внутрішнього відбивання. В роботі представлено розроблений та реалізований нами інтерференційний метод вимірювання фазових зсувів між ортогональними поляризаціями при повному внутрішньому відбиванні. Приведено результати експериментальних досліджень, які показали, що при повному внутрішньому відбиванні ортогональних лінійно-поляризованих компонент, поздовжній зсув між ними не супроводжується зміною різниці фази між ними. Цей результат дає позитивний прогноз для одночасного використання ортогональних лінійно поляризованих пучків у волоконно-оптичних лініях зв'язку.

КЛЮЧОВІ СЛОВА ефект Гуса-Хенхен, повне внутрішнє відбивання, ортогональні полярізації, волоконно-оптичні лінії зв'язку, поляризатор.